Dynamics of a dissociating gas
Part I Equilibrium flow

By M. J. LIGHTHILL
Department of Mathematics, University of Manchester

(*Received* 12 *October* 1956)

CONTENTS

1. INTRODUCTION

Atmospheric dissociation will be appreciable in the neighbourhood of projectiles travelling at speeds greater than 2 km/sec. This introductory paper on possible effects of dissociation on the airflow, and hence on the drag, stability and aerodynamic heating of such projectiles, is intended mainly as a source of ideas for later, more comprehensive investigations.

The problem of incorporating the effects of the large energy change involved in dissociation into the standard theory of gas flow appears at the same time so important and so formidable that it is worth approaching slowly. One may usefully begin, on both the theoretical and experimental sides, by eliminating the less essential complications which arise from the detailed composition of air, and studying the dynamics of a pure dissociating

diatomic gas. By keeping within bounds in this way the difficulty of imagining what is happening in the flow, one reduces the risk that some important feature will be missed.

The theoretical treatment of the dynamics of a pure dissociating gas which follows is concerned principally with properties at densities between 10^{-3} and 1 of N.T.P., and at temperatures such that dissociation occurs appreciably but ionization is negligible. For the gases, O_2 and N_2, which will be principally used for numerical illustration, this means temperatures in the approximate range 3000° K to 7000° K. Other gases suitable for pioneer experimental work on the problem and comparison with theory are the halogens, which already dissociate appreciably at 1000° K and so can be studied with lighter equipment. Thus, Britton, Davidson & Schott (1954) have used I_2, and Palmer (1955) Br_2.

The problem falls into three main parts, as follows.

(i) The theory of flow in which thermodynamic equilibrium is maintained everywhere; this is a good approximation to flow outside the boundary layer if the time scale for flow past the body is large compared with the time scale for dissociation or recombination. This theory is given in § 3, after the necessary equilibrium thermodynamics has been discussed in § 2.

(ii) The quasi-equilibrium theory of the transport properties, including radiative heat transfer as well as convective heat and momentum transfer in the boundary layer; this theory (to be given in Part II) is a good approximation if the time scale for diffusion across the boundary layer is large compared with the time scale for dissociation or recombination. Actually, the time scales for flow past the body and for diffusion across the boundary layer are the same (which is, indeed, what determines the thickness of the boundary layer), and so there is just one condition for theories (i) and (ii) to be valid.

(iii) The theory of flow in which this condition is not satisfied, so that large departures from equilibrium occur (not just the small ones supposed under heading (ii) to be responsible for the heat and momentum transport); this theory (to be given in Part III) includes the theory of the extended character of the shock wave and the effect of this on the flow behind it, and also the effect on boundary-layer behaviour of the delay in recombination of free atoms diffusing into the neighbourhood of the cooled wall.

The paper begins with a study (§ 2) of the equilibrium statistical thermodynamics of a pure dissociating gas. Here, an approximation is found which greatly simplifies the analysis and yet introduces only small errors for particular gases. One may speak of a hypothetical gas satisfying this approximate form of the thermodynamic equations as an 'ideal dissociating gas'. The properties of an ideal dissociating gas are given completely once three constants T_d, ρ_d and u_d (the 'characteristic' temperature, density and specific energy for dissociation) are given. Different pure dissociating gases differ in the values to be assigned to these constants, but otherwise (to the good approximation with which they can be treated as 'ideal' dissociating

gases) have all the same thermodynamics; a single theory, therefore, will do for all, whereas if the aproximation were not made separate calculations would need to be done for each gas.

Approximations equivalent to those in the thermodynamical theory of an ideal dissociating gas are made also in the discussions of quasi-equilibrium flow and flow involving large departures from equilibrium in Parts II and III. Physically, they amount always to taking the vibrational modes of motion of the molecules as everywhere excited to just half their full 'classical' energy content. At the high temperatures at which this would be expected to be a serious underestimate, the molecules have been so reduced in number by dissociation, and the energy absorbed in this process has been so large a fraction of the total internal energy, that the latter is in fact underestimated by a very few per cent. Under these circumstances the gain in simplicity well compensates for the loss in accuracy, as has been found many times before when hypothetical ideal fluids have been introduced in hydrodynamics.

Another reason why in this paper the author has avoided the complications due to the variation in degree of excitation of the vibrational mode of motion is that these complications were rather fully treated (in the absence of dissociation) in his recent survey article in the G. I. Taylor Anniversary Volume (Lighthill 1956). In the present paper the enquiry into the effects of molecular constitution on gas dynamics, begun in that article, is continued with a study of the effects of dissociation, but to simplify matters the concomitant effects of variation of vibrational excitation are here excluded.

The papers and books listed in the bibliographies have greatly assisted the author in preparing the three parts of this paper. However, like his other papers, it could never have been written without extensive private discussion and correspondence with friends. The help of Mr E. Wild has again been invaluable, and it is a pleasure to thank in addition Dr W. Chester, Mr N. C. Freeman, Dr A. G. Gaydon, Dr W. C. Griffith, Dr A. R. Kantrowitz, Dr L. Lees, Mr D. J. Lyons, Dr J. S. Rowlinson, Dr K. Stewartson, Dr P. Thompson, Mr A. K. Weaver, Dr M. D. Van Dyke, and Mr H. K. Zienkiewicz for many useful suggestions.

2. Equilibrium theory of a pure dissociating diatomic gas

2.1. *Law of mass action for dissociative equilibrium*

The law governing the equilibrium concentrations in a dissociative process

$$A_2 \rightleftharpoons A + A \tag{1}$$

is well known (see for example Fowler & Guggenheim 1939, §§ 502–508). We have

$$\frac{n_A^2}{n_{A_2}} = \frac{f_A^2}{f_{A_2}\epsilon^{D/kT}}, \tag{2}$$

where n_A is the number of A atoms in volume V at a given temperature T, and f_A is the partition function of A, namely the sum

$$\sum e^{-\epsilon/kT} \tag{3}$$

over all quantum states of the A atom in the volume V; n_{A_2} and f_{A_2} are defined similarly, but the energies ϵ in both f_A and f_{A_2} are commonly measured from the energy of the atom and molecule respectively when at rest in their ground states. The factor $e^{D/kT}$ (where D is the dissociation energy per molecule) is therefore attached to f_{A_2} to bring both sets of energies to a common origin. Equation (2) says really that the concentrations will adjust themselves in direct proportion to the number of states available at the given volume and temperature, bearing in mind the reduced availability of high-energy states which results from the Maxwell–Boltzmann distribution law.

The theory as described neglects complications due to gas imperfection, that is, contributions to the energy at any given instant from such interactions between molecules as are happening at that instant, which are associated with pressure reduction due to attraction between molecules and pressure increase due to overcrowding (that is, to reduced availability of translational states). The corrections for these effects, whose expression by means of a second virial coefficient may be extrapolated above the temperatures at which measurements have been made by the use of a Lennard–Jones (12, 6) potential (see for example Hirschfelder, Curtiss & Bird 1954) are of magnitude about $1/\rho$ or less, if the density ρ is expressed in gm/cm^3. We shall not be concerned in this paper with densities at which such a correction is appreciable.

The quantum states to be enumerated in (3) are combinations of translational, rotational, vibrational and electronic states, which can be regarded for practical purposes as independent of one another. (Nuclear states may be ignored, as any contribution to the partition function due to them will cancel in the ratio (2).) Using indices T, R, V and E for the four kinds of state, we have therefore

$$f_A = f_A^T f_A^E; \qquad f_{A_2} = f_{A_2}^T f_{A_2}^E f_{A_2}^R f_{A_2}^V. \tag{4}$$

2.2. *Detailed expressions for partition functions*

The translational partition function f_A^T is found by replacing the sum (3) by an integral over the classical 'phase space', cells of which of volume h^3 contribute one state each to the sum, as

$$f_A^T = \frac{(2\pi mkT)^{3/2}V}{h^3}, \tag{5}$$

where m is the mass of the A atom; clearly, f_{A_2} is the same with m replaced by $2m$. The rotational partition function is similarly found (a factor $\frac{1}{2}$ being inserted, however, to allow for the indistinguishability of the atoms) to be

$$f_{A_2}^R = \frac{1}{2}\frac{8\pi^2 IkT}{h^2} = \frac{1}{2}\left(\frac{T}{T_r}\right), \tag{6}$$

where I is the moment of inertia of the A_2 molecule. Equation (6) defines a 'characteristic temperature for rotation', T_r. The summand in (3) varies

gradually enough for the sum to be replaced by an integral as in (6) provided that $T \gg T_r$. For O_2, $T_r = 2{\cdot}07°$ K, and for N_2, $T_r = 2{\cdot}86°$ K, so that this requirement is amply satisfied in the present application.

The lower vibrational states of A_2 differ in energy from the gound state by 0, $h\nu$, $2h\nu$, ..., where ν is the frequency calculated classically from the mass m of the A atom and the curvature of the potential-energy curve at equilibrium. The vibrational partition function computed by assuming that the arithmetic progression of energy levels continues unchanged to infinity is

$$f^V_{A_2} = \frac{1}{1-e^{-h\nu/kT}} = \frac{1}{1-e^{-T_v/T}}, \tag{7}$$

where $T_v = h\nu/k$, the characteristic temperature for vibration, is 2230 °K for O_2 and 3340° K for N_2. More accurately, one may calculate f^V from the Morse (1929) energy levels of a molecule with dissociation energy D as

$$f^V_{A_2} = \sum_{0 \leqslant n < 2D/h\nu} \exp\left[-nh\nu\left\{1 - \frac{(n+1)h\nu}{4D}\right\}\Big/kT\right], \tag{8}$$

but the difference from (7) can be shown to be small when $T \ll D/k$, which is 59000° K for O_2 and 113000° K for N_2. (The same condition is amply adequate for the absence of any significant interaction between the rotational and vibrational degrees of freedom.)

The electronic partition functions f^E_A and $f^E_{A_2}$ consist normally of only a very few terms, since the higher electronic states are filled to an extent negligible from the thermodynamic point of view (although not from the spectroscopic). For oxygen, we may take

$$f^E_O = 5 + 3e^{-228/T} + e^{-327/T}, \qquad f^E_{O_2} = 3 + 2e^{-11300/T}, \tag{9}$$

if terms of order $e^{-23000/T}$ can be neglected. The values quoted arise from the fact that the ground state of oxygen is a triplet, states of weight 5, 3 and 1 (that is, spectroscopic terms $^3P_2$, $^3P_1$ and $^3P_0$) being energetically very close to one another; while the ground state ($^3\Sigma$) of O_2 is of weight 3 and the next state ($^1\Delta$), of weight 2, is not quite negligibly far away. (Note that at the temperatures ($> 2000°$ K) at which dissociation of O_2 is appreciable f^E_O is practically 9.)

For nitrogen, the electronic partition functions are still simpler, and

$$f^E_N = 4, \qquad f^E_{N_2} = 1, \tag{10}$$

if terms of order $e^{-28000/T}$ can be neglected.

Note that all the characteristic temperatures which have been quoted are known with considerable accuracy from absorption and emission spectra associated with transitions between the various states of the atom or molecule. Numerical values used here are all taken from Fowler & Guggenheim (1939) and Gaydon (1953). The only value which has been controversial until recently is the dissociation energy of N_2, but the value used (9·76 eV per molecule) is now firmly established.

2.3. *Equations of equilibrium in a hydrodynamically convenient form*

For hydrodynamical calculations it is convenient to express the results in terms of the density, namely

$$\rho = \frac{m(n_A + 2n_{A_2})}{V}, \tag{11}$$

and the proportion by mass of A atoms in the mixture, namely

$$\alpha = \frac{n_A}{n_A + 2n_{A_2}}. \tag{12}$$

Then equation (2), with all the results of equations (4) to (10) substituted in it, becomes

$$\begin{aligned} \frac{\alpha^2}{1-\alpha} &= \frac{n_A^2}{2n_{A_2}(n_A + 2n_{A_2})} = \frac{m}{2\rho V}\frac{n_A^2}{n_{A_2}} \\ &= \frac{e^{-D/kT}}{\rho}\left\{(\tfrac{1}{2}m)\frac{(\pi mkT)^{3/2}}{h^3}\left(\frac{2T_r}{T}\right)(1-e^{-T_v/T})\frac{(f_A^E)^2}{(f_{A_2}^E)}\right\} \\ &= \frac{\rho_d}{\rho}e^{-D/kT}, \end{aligned} \tag{13}$$

where $T_d = D/k$ is a characteristic temperature for dissociation, and ρ_d, defined as the contents of the curly brackets in (13), is a characteristic density.

	T_d (° K)	ρ_d (gm/cm^3) when T (° K) is 1000	2000	3000	4000	5000	6000	7000
Oxygen	59000	145	170	166	156	144	133	123
Nitrogen	113000	113	135	136	133	128	123	118

Table 1

Table 1 gives T_d, and also ρ_d as a function of T, for both oxygen and nitrogen. It will be seen that the variation of ρ_d over the large temperature range from 1000° to 7000° is very slight for both gases, especially when compared with the enormous variation of $e^{-T_d/T}$ in this range, and for practical purposes the useful simplification of regarding ρ_d as a constant (say, 150 for oxygen and 130 for nitrogen) should lead to negligible errors. This approximation will be made throughout what follows.

The rather close agreement between the values of ρ_d for the two gases is due to an accidental cancelling: the abundance of rotational and vibrational states in O_2 as compared with N_2 would make ρ_d substantially smaller for oxygen than for nitrogen, were it not that the abundance of electronic (and, to a minor extent, of translational) states in O as compared with N works the other way.

Now, for atmospheric values of the density ρ, ρ_d/ρ is at least 10^5. This consequence of the far greater number of translational states available to the gas as A than as A_2 at these densities explains why dissociation first

sets in at temperatures rather small compared with the characteristic temperature T_d. Thus, for $\rho_d/\rho = 10^5$, (13) shows that α is already 0·05 (5% dissociation) when $T/T_d = 0{\cdot}057$, and α is 0·95 (95% dissociation) when $T/T_d = 0{\cdot}116$. For densities typical of the upper atmosphere, with (say) $\rho_d/\rho = 10^7$, these values of T/T_d would be reduced to 0·045 and 0·076 respectively. Figure 1 is a diagram in which by use of a reciprocal temperature scale it has been made easy to read off the degree of dissociation α for any values of T/T_d and ρ/ρ_d.

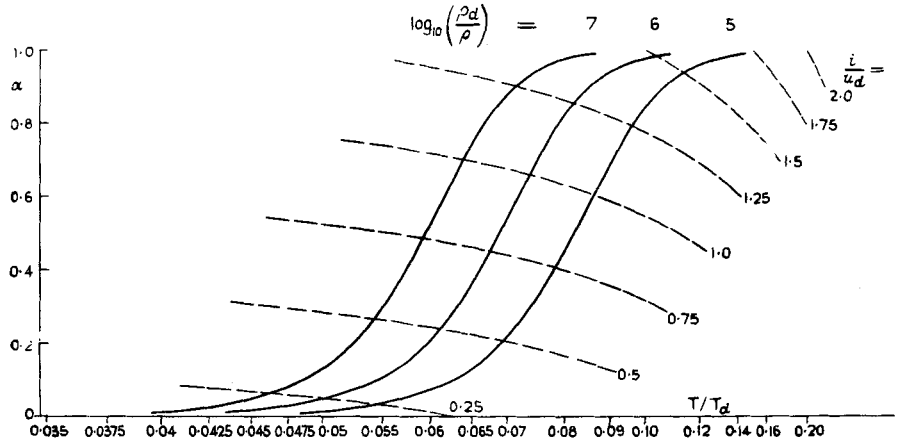

Figure 1. Plain lines give α (the proportion by mass of free atoms in an ideal dissociating gas) against T/T_d for $\log_{10}(\rho_d/\rho) = 7, 6, 5$. The diagram is such that linear interpolation with respect to $\log_{10}(\rho_d/\rho)$ at any horizontal level is accurate. For oxygen, $\rho_d = 150$ gm/cm^3 and $T_d = 59000°$ K. For nitrogen, $\rho_d = 130$ gm/cm^3 and $T_d = 106000°$ K. Broken lines are lines of constant i/u_d, the enthalpy divided by the heat of dissociation. For these, linear interpolation in the vertical direction is almost accurate.

We shall need also the equation of state of the gas mixture. The pressure p is equal to the volume density of translational momentum transfer in a given direction per unit time, which occurs at an average rate kT per atom or molecule, giving

$$p = \frac{kT(n_A + n_{A_2})}{V} = \frac{kT(1+\alpha)(n_A + 2n_{A_2})}{2V} = \frac{k}{2m}\rho T(1+\alpha). \qquad (14)$$

Here $k/2m$ is often written as R; it is the gas constant per gram of A_2. (Multiplied by $1+\alpha$, it is the gas constant per gram of A and A_2 mixed in the proportions $\alpha:(1-\alpha)$ by mass.) It may be more convenient here to introduce a characteristic pressure for dissociation,

$$p_d = \left(\frac{k}{2m}\right)\rho_d T_d = \left(\frac{D}{2m}\right)\rho_d, \qquad (15)$$

in terms of which (14) becomes

$$\frac{p}{p_d} = \left(\frac{\rho}{\rho_d}\right)\left(\frac{T}{T_d}\right)(1+\alpha). \qquad (16)$$

Values of p_d are given in table 3 below.

We need also an expression for the internal energy as a function of temperature and composition. This is obtained from the partition functions of § 2.2. The total internal energy U in volume V is

$$U = kT^2\left\{n_A \frac{\partial}{\partial T}\log f_A + n_{A_2}\frac{\partial}{\partial T}\log f_{A_2}\right\} + \tfrac{1}{2}Dn_A, \tag{17}$$

since the average energy per A atom is

$$\frac{\sum \epsilon e^{-\epsilon/kT}}{\sum e^{-\epsilon/kT}} = kT^2\frac{\partial}{\partial T}\log f_A, \tag{18}$$

and similarly with A_2; the term $\frac{1}{2}Dn_A$ is needed because in f_A and f_{A_2} the zeros of energy are different, two atoms of A at their zero of energy having energy D more than a molecule of A_2 at its zero.

Now, to be consistent with the approximation ρ_d = constant suggested above (which implies $f_A^2 \propto f_{A_2}$) the curly bracket in (17) should be taken proportional to $n_A + 2n_{A_2}$, and since f_A is almost exactly proportional to $T^{3/2}$, the coefficient of $n_A + 2n_{A_2}$ might reasonably be taken as $3/(2T)$, leading to the approximation

$$U = \tfrac{3}{2}kT(n_A + 2n_{A_2}) + \tfrac{1}{2}Dn_A. \tag{19}$$

This could be physically interpreted by saying that atoms and molecules both have average translational energy $\frac{3}{2}kT$, but that molecules have in addition an average rotational and vibrational energy of about $\frac{3}{2}kT$ (it varies at most between kT and $2kT$), electronic contributions being neglected. Table 2 gives the accurate values of the coefficients of n_A and $2n_{A_2}$ in $(U - \frac{1}{2}Dn_A)/kT$, obtained from (17), for both oxygen and nitrogen, for comparison with 1·5, the approximate value of each coefficient suggested by (19). At first sight the variations might be thought important, but in

	T (° K)	1000	2000	3000	4000	5000	6000	7000
Coefficient of n_A	Oxygen	1·60	1·55	1·54	1·53	1·52	1·52	1·51
	Nitrogen	1·50	1·50	1·50	1·50	1·50	1·50	1·50
Coefficient of $2n_{A_2}$	Oxygen	1·38	1·54	1·62	1·68	1·72	1·75	1·77
	Nitrogen	1·31	1·44	1·52	1·57	1·60	1·62	1·64

Table 2

practice they are swamped by the term involving the large dissociation energy D. Accordingly (19) will be used throughout what follows. It gives for the energy per unit mass u, commonly used in hydrodynamics, the expression

$$u = \frac{U}{\rho V} = \frac{3k}{2m}T + \frac{D}{2m}\alpha. \tag{20}$$

In terms of a characteristic energy per unit mass

$$u_d = \frac{D}{2m} \tag{21}$$

(the dissociation energy per gram of A_2), equation (20) becomes

$$\frac{u}{u_d} = 3\frac{T}{T_d} + \alpha. \tag{22}$$

Values of p_d, u_d and $u_d^{1/2}$ for oxygen and nitrogen are given in table 3.

	p_d (atmospheres)	u_d (k cal/gm)	u_d (cm^2/sec^2)	$v_d = u_d^{1/2}$ (km/sec)
Oxygen	$2{\cdot}3\times10^7$	3·67	$1{\cdot}53\times10^{11}$	3·9
Nitrogen	$4{\cdot}1\times10^7$	8·02	$3{\cdot}35\times10^{11}$	5·8

Table 3

Here, $u_d^{1/2}$ ($= v_d$, say) is a characteristic velocity for dissociation; fluid with this velocity has enough kinetic energy to provide half the energy required to dissociate it completely. Note also that $p_d = \rho_d v_d^2$ so that p_d is typical of the pressures obtained by stopping a flow at velocity v_d and density ρ_d. It exceeds the pressures which will be found in a real flow with velocity v_d, by the same large factor by which ρ_d exceeds the real density ρ.

2.4. *Summary of thermodynamics of an ideal dissociating gas*

We shall use the expression 'ideal dissociating gas' to denote a gas for which equations (13), (16) and (22) hold with ρ_d (and hence also p_d) replaced by a constant. For calculations concerning changes in such a gas between different states of equilibrium, it may be convenient to use T_d, ρ_d, p_d and u_d as the units, respectively, of temperature, density, pressure and specific internal energy (in a flow problem this implies using $u_d^{1/2} = v_d$ as the unit of velocity). In these units the fundamental equations (13), (16) and (22) take the simple forms

$$\frac{\alpha^2}{1-\alpha} = \left(\frac{1}{\rho}\right)e^{-1/T}, \qquad p = \rho T(1+\alpha), \qquad u = 3T+\alpha. \tag{23}$$

The specific enthalpy, which plays an important part in steady flow problems, has the value

$$i = u + \frac{p}{\rho} = (4+\alpha)T + \alpha \tag{24}$$

when measured with u_d as unit. Curves of constant i are included in figure 1, so that the enthalpy required to produce a given degree of dissociation at a given density can be read off conveniently.

The specific entropy S will also be needed. It is obtained most simply from the relation

$$dS = \frac{du + p\,d(\rho^{-1})}{T} = \frac{3dT + d\alpha + \rho T(1+\alpha)d(\rho^{-1})}{T}$$

$$= \frac{3dT}{T} + \log\frac{1-\alpha}{\rho\alpha^2}\,d\alpha - \frac{(1+\alpha)d\rho}{\rho}. \tag{25}$$

Hence, by integration,

$$S = 3\log T + \alpha(1 - 2\log\alpha) - (1-\alpha)\log(1-\alpha) - (1+\alpha)\log\rho + \text{const.} \quad (26)$$

The value of the constant can be found from the detailed expressions for the partition functions, but will not be needed in the present paper, since no chemical changes other than dissociation and reassociation are considered. Whenever numerical values of S are given, the constant in (26) has simply been taken as zero. Note that the unit in which S is measured in (26) is $u_d/T_d = k/2m$, simply the gas constant per gram of A_2.

The properties of the ideal dissociating gas may be conveniently summarized in a classical enthalpy–entropy diagram (Mollier diagram) such as figure 2, which shows the lines of constant temperature, pressure, density and composition in the region of the diagram corresponding to pressures between (3×10^{-9}) and (3×10^{-6}) times the characteristic pressure. These were obtained by selecting pairs of values of α and ρ, determining T from (23) and then i and S from (24) and (26), and also by selecting pairs of values of p, T, determining α as $(1+pT^{-1}\exp T^{-1})^{-1/2}$ and using (23), (24) and (26) to obtain i and S as before. Note how the enthalpy on the isothermals rises as the gas dissociates with decreasing pressure. This sloping up of the isothermals causes the isobars to be unusually straight in the region of dissociation, since the slope $di/dS = T$ of an isobar varies only slowly along it. The lines of constant density show a similar behaviour.

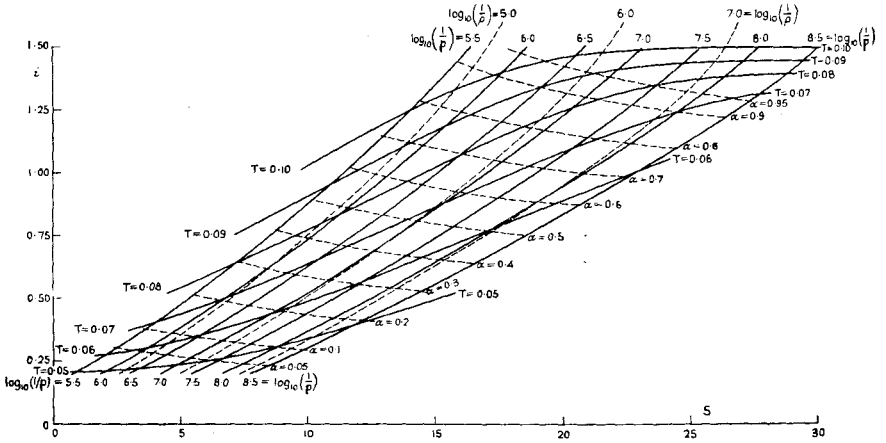

Figure 2. Enthalpy–entropy diagram for ideal dissociating gas (units as in § 2.4).

It is outside the scope of this paper to consider the behaviour of dissociating gases in internal aerodynamics, and therefore the 'Fanno' lines representing flow in ducts of constant area have not been included in figure 2, though they could easily be obtained. One may remark, however, that the properties exhibited in figure 2 make a dissociating gas an attractive possibility for heat engines. Thus, a closed-cycle gas turbine operating in

a large temperature range, which may be desirable for utilizing the energy output of a nuclear reactor, may in principle reach a high thermal efficiency with a gas in which the temperature increases so slowly along the isobars. At the sort of temperatures that could be conveniently dealt with, a gas like I_2 with $T_d = 18000°$ K might be suitable. By operating up to 0·08 or 0·09 of this characteristic temperature one might achieve the favourable general shape of the steam-turbine cycle with a temperature range many times as great.

Note that, as $\alpha \to 0$ at low temperatures, the ideal dissociating gas becomes a perfect gas with constant specific heats, in the ratio $\gamma = c_p/c_v = \frac{4}{3}$. (Physically, this is because the vibrational degrees of freedom are taken to be half-excited even at low temperatures.) It might be thought desirable for the ideal dissociating gas to have $\gamma \to \frac{7}{5}$ at low temperatures, but, since projectiles travelling at speeds like those mentioned in § 1 cannot in practice have their surface kept below 1000° K, $\frac{4}{3}$ is a reasonably realistic low-temperature limit for γ in the field of flow around such a projectile.

3. Equilibrium flow theory for an ideal dissociating gas

3.1. *Requirements for equilibrium flow*

We consider now the flow of the ideal dissociating gas of § 2 under conditions in which to a good approximation an equilibrium state is maintained at all points. This means (i) that the state of each portion of fluid changes slowly compared with the relaxation frequencies of all the processes involved in maintaining equilibrium, and (ii) that there is no transport of momentum or heat, or significant interdiffusion of atoms and molecules, across surfaces moving with the mass velocity of the fluid. (In Part II we shall consider flows in which restriction (ii) is removed but (i) is retained, and in Part III flows in which both are removed.)

It is well known that the equations governing such reversibly-adiabatic gas motions do not always possess continuous solutions, but that solutions involving where necessary a discontinuity or 'shock wave', across which irreversible changes of state occur but mass, momentum and energy are conserved, can always be set up, and these correspond well with what is observed. Energy dissipation occurs within shock waves, but the time spent by any fluid particles within the region of dissipation is not great compared with the relaxation times just mentioned (except for very weak shock waves indeed), and, whenever the distance travelled during such a time is small compared with the basic length scales of the flow, the solutions which treat the shock wave as a discontinuity are useful. These solutions are considered in this section as well as the continuous ones. Indeed, since the first change experienced by the air as a supersonic projectile approaches is passage through a shock wave, the conditions governing this change will be studied first.

3.2. *Conditions behind a shock wave*

In a frame of reference in which the shock wave is stationary, the Rankine–Hugoniot equations of conservation of mass, momentum and energy across it are

$$\rho_0 v_{n0} = \rho_1 v_{n1}, \tag{27}$$

$$\mathbf{v}_{t0} = \mathbf{v}_{t1}, \tag{28}$$

$$p_0 + \rho_0 v_{n0}^2 = p_1 + \rho_1 v_{n1}^2, \tag{29}$$

$$i_0 + \tfrac{1}{2} v_{n0}^2 = i_1 + \tfrac{1}{2} v_{n1}^2, \tag{30}$$

where suffix 0 denotes conditions ahead of the shock, suffix 1 conditions behind it, and v_n and $\mathbf{v}_t$ denote velocity components normal and tangential to it.

With atmospheric temperatures ahead of the shock, dissociation can be appreciable only if v_{n0} is large—so large, in fact, that the terms p_0 in (29) and i_0 in (30) can be neglected. Thus, figures 1 and 2 show that dissociation is not very important unless $i_1 > 0{\cdot}25$, so that by (30) $i_0 + \frac{1}{2} v_{n0}^2 > 0{\cdot}25$. But $i_0 < 0{\cdot}02$ if the temperature T_0 ahead of the shock is less than $0{\cdot}006$ (this fraction of T_d is 350° K for oxygen and 640° K for nitrogen), so that in this case i_0 is already small compared with $\frac{1}{2} v_{n0}^2$ for the rather small amount of dissociation implied by the selected value of i_1, and becomes quite negligible for larger amounts. The ratio of p_0 to $\rho_0 v_{n0}^2$ is still smaller.

Accordingly, the 'strong-shock approximation' of neglecting i_0 and p_0 will here be made, and (27), (29) and (30) written as

$$\rho_0 v_{n0} = \rho_1 v_{n1}, \qquad \rho_0 v_{n0}^2 = p_1 + \rho_1 v_{n1}^2, \qquad \tfrac{1}{2} v_{n0}^2 = i_1 + \tfrac{1}{2} v_{n1}^2. \tag{31}$$

It follows from (31) by elimination of v_{n0} and v_{n1} that the density-ratio at the shock wave is

$$\frac{\rho_1}{\rho_0} = \frac{i_1}{\frac{1}{2}(p_1/\rho_1)} - 1 = \frac{u_1}{\frac{1}{2}(p_1/\rho_1)} + 1 = K, \tag{32}$$

where K is one plus the ratio of the total internal energy of the gas to the energy of the translational motion in any one particular direction. Figure 3 gives graphs of

$$K = \frac{3T_1 + \alpha}{\frac{1}{2} T_1 (1+\alpha)} + 1 = 7 + \frac{2\alpha}{1+\alpha}\left(\log \frac{1-\alpha}{\rho_1 \alpha^2} - 3\right) \tag{33}$$

as a function of α for different values of $\log_{10}(1/\rho_1)$; since interpolation with respect to $\log_{10}(1/\rho_1)$ is linear for fixed α (that is, at any horizontal level), only two curves have been drawn.

In terms of K, the pressure and enthalpy behind the shock are given by (31) as

$$p_1 = \left(1 - \frac{1}{K}\right)\rho_0 v_{n0}^2, \qquad i_1 = \left(1 - \frac{1}{K^2}\right)(\tfrac{1}{2} v_{n0}^2). \tag{34}$$

Note that over 98% of the kinetic energy of the fluid approaching the shock wave is converted directly into enthalpy by it.

To determine conditions behind a shock wave given the density and velocity ahead of it, one may first use (34) to give i_1 correct to 1 or 2%. Assuming a rough value of K of say 10 or 12, one then determines from figure 1 the value of α corresponding to the enthalpy i_1 and to a density $K\rho_0$, and hence from figure 3 (using this α and the same value for the density) an improved approximation to K. If the first guess of K was badly out the process may then be repeated to improve the approximation, but otherwise this is unnecessary.

For example, if in the units here used $v_{n0} = 1{\cdot}2$ and $\rho_0 = 2 \times 10^{-7}$, then $i_1 = 0{\cdot}72$ and, to a rough approximation (taking $K = 12$), $\rho_1 = 2{\cdot}4 \times 10^{-6}$ and $\log_{10}(1/\rho_1) = 5{\cdot}62$. From figure 1 for these values $\alpha = 0{\cdot}42$, whence from figure 3 to a better approximation $K = 13{\cdot}2$, giving $\rho_1 = 2{\cdot}64 \times 10^{-6}$ and $\log_{10}(1/\rho_1) = 5{\cdot}58$. If this new value is used instead of 5·62, the values obtained for α and K are unchanged in the last figure quoted.

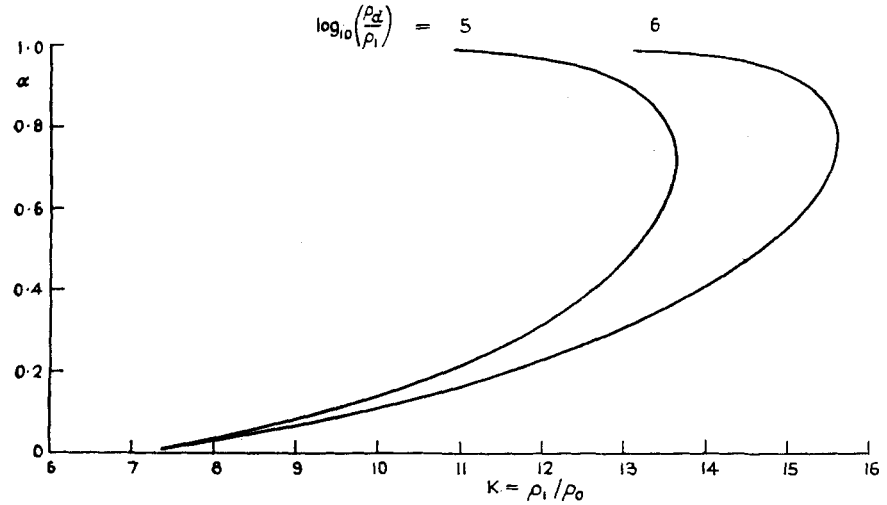

Figure 3. Density-ratio K at a shock wave, as a function of ρ_1 and α, the density and degree of dissociation behind it. Linear interpolation with respect to $\log_{10}(\rho_d/\rho_1)$ at any horizontal level is accurate.

Although we shall not use them in this paper, it is valuable in more accurate calculations to have available the second approximation to the shock wave equations (32) and (34). This takes into account the terms p_0 and i_0 in (29) and (30) but neglects their squares. If the gas ahead of the shock is taken as an ideal diatomic gas with velocity of sound $a_0 = \sqrt{(7p_0/5\rho_0)}$, then these second approximations are

$$\frac{\rho_1}{\rho_0} = K\left\{1 - \frac{5(6K-1)}{7(K-1)}\,\frac{a_0^2}{v_{n0}^2}\right\}, \qquad \frac{p_1}{\rho_0 v_{n0}^2} = 1 - \frac{1}{K} + \frac{5(K^2-7K+1)}{7K(K-1)}\,\frac{a_0^2}{v_{n0}^2},$$

$$\frac{i_1}{\tfrac{1}{2}v_{n0}^2} = 1 - \frac{1}{K^2} + 5\left\{1 - \frac{2(6K-1)}{7K^2(K-1)}\right\}\frac{a_0}{v_{n0}^2}.$$

The effects on ρ_1 and i_1 are appreciable (around 5% even for $v_{n0}/a_0 = 10$) but that on p_1 is very small (less than 0·4% under the same condition).

3.3. *Effects of non-uniformity of shock wave strength*

Any projectile travelling at speed V must have a shock wave ahead of it which is normal to the direction of motion at one point at least (since an ideally sharp apex or edge in front of the projectile could not be used in practice). At this point $v_{n0} = V$ and hence i_1 is very nearly $\frac{1}{2}V^2$. It follows from figure 1 that about 5% dissociation will occur behind this point on the shock wave when $V \doteqdot 0{\cdot}7$, 25% when $V \doteqdot 1{\cdot}0$, 50% when $V \doteqdot 1{\cdot}3$, 75% when $V \doteqdot 1{\cdot}5$ and 95% when $V \doteqdot 1{\cdot}6$, the unit for V being of course v_{ll}. These are only rough values; the variation with density of the dissociation produced can be seen from the figure.

At other points on the shock wave, where it is inclined at an angle η to the direction of motion, $v_{n0} = V\sin\eta$, and the enthalpy behind the shock wave is reduced. Thus, there is less energy dissipation in these weaker portions of shock wave, where accordingly the entropy increase is less. The entropy gradient behind the shock wave is easily inferred from (34). If dS_1 is the difference in entropy behind elements of shock wave with a difference dv_{n0} in upstream normal velocity, then

$$\begin{aligned} T_1\,dS_1 &= di_1 - \frac{1}{\rho_1}dp_1 \\ &= \left(1-\frac{1}{K^2}\right)v_{n0}\,dv_{n0} + \frac{v_{n0}^2\,dK}{K^3} - \frac{1}{K\rho_0}\left\{2\left(1-\frac{1}{K}\right)\rho_0\,v_{n0}\,dv_{n0} + \right. \\ &\qquad \left. + \frac{\rho_0\,v_{n0}^2\,dK}{K^2}\right\} \\ &= \left(1-\frac{1}{K}\right)^2 v_{n0}\,dv_{n0}, \end{aligned} \tag{35}$$

the terms due to the variability of K cancelling out.

This variation of entropy behind the shock leads to the presence of vorticity. At a point P where the two 'principal curvatures' of the shock surface are κ_a and κ_b (with curvatures taken positive when they are convex to the oncoming flow), let suffix a signify components parallel to the line of curvature through P which has curvature κ_a, and suffix b similarly. Then at a point on the shock surface near P, whose separation from P has components δx_a, δx_b, the velocities differ from those at P by the amounts

$$\delta v_{n0} = -v_a\kappa_a\,\delta x_a - v_b\kappa_b\,\delta x_b, \quad \delta v_a = v_{n0}\kappa_a\,\delta x_a, \quad \delta v_b = v_{n0}\kappa_b\,\delta x_b. \tag{36}$$

But the equation of momentum in the continuous flow behind the shock wave may be written in terms of the vorticity $\boldsymbol{\omega} = \operatorname{curl}\mathbf{v}$ as

$$\boldsymbol{\omega}\wedge\mathbf{v} + \nabla(\tfrac{1}{2}v^2) + \frac{1}{\rho}\nabla p = 0, \tag{37}$$

where the first two terms are a familiar form of the acceleration of a fluid element in steady flow. This, combined with the energy equation

$$\tfrac{1}{2}v^2 + i = \text{constant}, \tag{38}$$

gives

$$\boldsymbol{\omega}\wedge\mathbf{v} = \nabla i - \frac{1}{\rho}\nabla p = T\nabla S. \tag{39}$$

Now by (36) the vorticity component normal to the shock surface vanishes; thus

$$\omega_n = \frac{\partial v_a}{\partial x_b} - \frac{\partial v_b}{\partial x_a} = 0. \tag{40}$$

Hence, resolving (39) in the a and b directions (assumed such that the a, b and n directions form a right-handed system),

$$\omega_{b1} v_{n1} = T_1 \frac{\partial S_1}{\partial x_a}, \qquad -\omega_{a1} v_{n1} = T_1 \frac{\partial S_1}{\partial x_b}. \tag{41}$$

From (41), (35), (36) and (27),

$$\begin{aligned} \omega_{b1} &= \frac{1}{v_{n1}} T_1 \frac{dS_1}{dv_{n0}} \frac{\partial v_{n0}}{\partial x_a} \\ &= -\frac{1}{v_{n1}} \left(1 - \frac{1}{K}\right)^2 v_{n0} v_a \kappa_a \\ &= -\frac{(K-1)^2}{K} v_a \kappa_a, \end{aligned} \tag{42}$$

and, similarly,

$$\omega_{a1} = +\frac{(K-1)^2}{K} v_b \kappa_b. \tag{43}$$

Thus, the vorticity component in either of the two principal directions of curvature of the shock surface is equal to the curvature in the direction at right angles, times the tangential velocity component, also in that direction, times a factor $(K-1)^2/K$, which for a dissociating gas is rather large (figure 3).

Results like this are usually stated for two-dimensional or axisymmetrical flow; these cases are simpler because the velocity component in one of the two principal directions of curvature vanishes. It may be useful, however, to have a more general type of result on record. Equations (42) and (43) are also completely general with respect to the thermodynamic properties of the gas; only the 'strong-shock' approximation has been used in deriving them.

3.4. *Properties of isentropic changes*

In the type of flow described in § 3.1, fluid particles undergo isentropic changes as they move along streamlines behind the front shock wave (at least, until they encounter another shock wave), although the entropy S has different values on different streamlines. The character of the flow changes when the fluid speed exceeds the local speed of sound, whose square is equal to the derivative of pressure with respect to density at constant entropy, even when propagation occurs in a region of varying entropy. Both these facts make it necessary to study isentropic changes in detail.

The general character of these changes can be seen from figure 2, two points being particularly worthy of notice. The change in i for a given

change in pressure is smaller than in most gases. In fact, at constant entropy

$$\frac{d\log i}{d\log p} = \frac{p}{i}\frac{di}{dp} = \frac{p}{i\rho} = \frac{2}{K+1}. \tag{44}$$

In the region of dissociation this is of the order of $\frac{1}{7}$, only half of its value for an ideal diatomic gas. Hence changes in enthalpy, and so also of the fluid speed

$$v = \sqrt{(V^2 - 2i)}, \tag{45}$$

with changes in pressure, are reduced when dissociation or reassociation is occurring. This is because the translational energy of the molecules is a reduced fraction of the total enthalpy.

Again, the change in $\log p$ with $\log\rho$ at constant entropy is slower for intermediate α than for either an ideal diatomic gas or a gas with constant adiabatic index $\frac{4}{3}$ (the limit of our ideal gas as $\alpha \to 0$), or a monatomic gas ($\alpha \to 1$). In fact the adiabatic index

$$\gamma = \frac{d\log p}{d\log\rho} = \frac{a^2}{p/\rho}, \tag{46}$$

from which the speed of sound a can be inferred, falls to around 1·2 in the region of dissociation. For by putting $dS = 0$ in (25), and using (23) with ρ expressed in terms of T and α, we can show that

$$\gamma = 1 + \frac{2T + \dfrac{2+3\alpha^2-\alpha^3}{\alpha(1-\alpha^2)}\,T^2}{1 + \dfrac{3(2-\alpha)}{\alpha(1-\alpha)}\,T^2}. \tag{47}$$

From table 4, which gives $\gamma - 1$ for different values of α, it is clear that, for the values of T of interest here (say, between 0·04 and 0·10), $(\gamma - 1)$ falls well below both its extreme values for all the intermediate values of α which are quoted.

α	0	0·1	0·2	0·3	0·4	0·5
$\gamma-1$	$\frac{1}{3}$	$\frac{2T+20{\cdot}5T^2}{1+63{\cdot}3T^2}$	$\frac{2T+11T^2}{1+33{\cdot}7T^2}$	$\frac{2T+8{\cdot}2T^2}{1+24{\cdot}3T^2}$	$\frac{2T+7{\cdot}2T^2}{1+20T^2}$	$\frac{2T+7{\cdot}0T^2}{1+18T^2}$
α		0·6	0·7	0·8	0·9	1·0
$\gamma-1$		$\frac{2T+7{\cdot}5T^2}{1+17{\cdot}5T^2}$	$\frac{2T+8{\cdot}8T^2}{1+18{\cdot}6T^2}$	$\frac{2T+11{\cdot}8T^2}{1+22{\cdot}5T^2}$	$\frac{2T+21{\cdot}6T^2}{1+36{\cdot}7T^2}$	$\frac{2}{3}$

Table 4

This behaviour of γ is not unrelated to the behaviour of K shown in figure 3. In fact, it follows from (44) that in a change at constant entropy,

$$\gamma = \frac{d\log p}{d\log\rho} = \frac{K+1}{K-1}\,\frac{d\log p - d\log i}{d\log\rho} = \frac{K+1}{K-1}\,\frac{d\log\rho - d\log(\frac{1}{2}K+\frac{1}{2})}{d\log\rho}$$
$$= \frac{K+1-dK/d\log\rho}{K-1}, \tag{48}$$

which may be compared with the relationship $\gamma = (K+1)/(K-1)$ for a gas with constant specific heats. The actual expression for the isentropic derivative $dK/d\log\rho$ is algebraically complicated but it can be seen from figures 2 and 3 to be numerically small for $\alpha < 0{\cdot}9$, so that the fall of γ to a minimum for intermediate α proceeds in parallel with the rise of K to a maximum for these α.

The square of the local Mach number immediately behind a shock wave, by (46) and (34), is

$$\frac{v_{n1}^2+v_{t1}^2}{\gamma p_1/\rho_1} = \frac{(v_{n0}^2/K^2)+v_{t0}^2}{\gamma(1-K^{-1})\rho_0 v_{n0}/K\rho_0} = \frac{1+K^2\cot^2\eta}{\gamma(K-1)}, \tag{49}$$

since $v_{n0} = V\sin\eta$ and $v_{t0} = V\cos\eta$. For a dissociating gas, then, this number is small (around 0·07) behind the normal part of the shock wave (where $\eta = \frac{1}{2}\pi$) but rises to unity where

$$\eta = \cot^{-1}\left\{\frac{\gamma(K-1)-1}{K^2}\right\}^{1/2}, \tag{50}$$

which for $\gamma = 1{\cdot}2$ and $K = 12$ (say) is 73·8°. Although the sonic line starts on a portion of shock wave inclined rather steeply to the flow, where the pressure is

$$p_1 = \left(1-\frac{1}{K}\right)\rho_0 V^2\sin^2\eta = \frac{K}{K+\gamma+1}\rho_0 V^2, \tag{51}$$

it ends at a point farther round the body, where the pressure (estimated from (44) by taking K constant) is about

$$\left(1-\frac{1}{K}\right)\left\{\left(1-\frac{1}{K^2}\right)\left(1+\frac{\gamma}{K+1}\right)\right\}^{-(K+1)/2}\rho_0 V^2. \tag{52}$$

For $\gamma = 1{\cdot}2$ and $K = 12$, the pressure (51) is $0{\cdot}845\rho_0 V^2$ and the pressure (52) is $0{\cdot}540\rho_0 V^2$.

3.5. *Flow about bluff bodies: approximations of Newtonian type*

The aerodynamic problems we shall consider will be concerned mostly with flow about bluff bodies (with the sphere as the typical body), partly because it seems clear that the flow about a projectile must at least start by negotiating a more or less bluff nose.

The theories of flows about bluff bodies at very high Mach number which are mentioned in the literature have been related by most authors in a somewhat far-fetched manner to a discussion by Newton (1687). Having no empirically-based knowledge of gaseous structure, Newton postulated a gas which we should now describe as having negligible thermal motions and very large mean free path and whose molecules collide inelastically with a solid surface. This gives a surface pressure of $\rho_0 V^2\sin^2\chi$, where χ is the angle between the surface and the direction of motion; all the momentum flux normal to a surface element is communicated directly to the surface. The reflection condition is satisfied if particles hitting the surface are adsorbed and later evaporate at the temperature of

the surface with energy small compared with $V^2 \sin^2\chi$. Cooled bodies may therefore satisfy the Newtonian assumptions at Mach numbers so large that thermal motions in the undisturbed atmosphere are negligible, but only if the density is so small that the mean free path is comparable with the body size. The last restriction is a severe one, and applies only at extreme altitudes, where the drag and heat transfer are not very important.

In the more interesting class of flows in which the mean free path is small compared with the size of the body, no plausible reason why the Newtonian rarefied-gas formula might be applicable has ever been advanced, but the prestige of Newton's name has been regarded by some scientists as an adequate substitute for a theory. (Newton actually gave a different argument, and a different answer, for denser fluids; although these were incompatible with our present knowledge of the mechanics of fluids, it is significant that he did not himself expect the rarefied-gas formula to be applicable.)

At the front stagnation point the pressure is equal to the stagnation pressure appropriate to the conditions behind the normal part of the shock To a good approximation, by (49), the flow here may be regarded as incompressible, and so, by (34) with $v_{n0} = V$, this stagnation pressure is

$$p_1 + \tfrac{1}{2}\rho_1 v_{n1}^2 = \left(1 - \frac{1}{K}\right)\rho_0 V^2 + \tfrac{1}{2}(K\rho_0)\left(\frac{V}{K}\right)^2$$
$$= \left(1 - \frac{1}{2K}\right)\rho_0 V^2, \tag{53}$$

a value only slightly below the 'Newtonian' value $\rho_0 V^2$. Lees (1955) suggests an empirical law

$$p = \left(1 - \frac{1}{2K}\right)\rho_0 V^2 \sin^2\chi \tag{54}$$

for the surface pressure distribution, in which the Newtonian formula is multiplied by a constant factor to make it accurate at the stagnation point, and in this way obtains good agreement with experimental pressure distributions on spheres, and cones of 40° semi-angle with spherical tips, in air flows at $M = 5{\cdot}8$, as observed by Oliver (1956). Such a formula could reasonably be used for extrapolation to when dissociation is present only if it had some plausible theoretical basis. This seems to be wanting. One can hardly regard the flow normal to a surface element (with velocity $V \sin\chi$) as independent of the flow tangential to it, which completely alters the streamline pattern on which the calculation of pressure recovery in (53) is based, as well as introducing important centrifugal pressure gradients.

A quite different approach was set out in a paper by Ivey, Klunker & Bowen (1948) and anticipated in a brief discussion by Busemann (1933). The approach has been used and further discussed by Grimminger, Williams & Young (1950), who call it 'the hypersonic approximation', and by Van Dyke (1954), who calls it the 'Newtonian-plus-centrifugal' theory. More recently, Chester (1956) and Freeman (1956) have both reconsidered the approach and pushed it to a second approximation.

This approach first assumes the Mach number so great that the strong-shock approximation can be used (as we did already in § 3.2) and then approximates further by taking K large. This may be regarded as beginning an expansion in inverse powers of K, or (speaking more accurately) a successive-approximation procedure in which the first approximation is the solution with $K = \infty$. Since K, as we have seen, is large for a dissociating gas, such a procedure is particularly attractive when dissociation occurs. But, as we shall see, it leads to difficulties for certain body shapes, principally due to uncertainty about the nature of the limiting flow for $K = \infty$.

Since for $K = \infty$ the density behind the shock wave is an infinite multiple of the density ahead of it, while the velocity component tangential to the shock wave is unchanged, the streamtube area might be expected to become zero on passage through the oblique parts of the shock wave. In this case the shock wave would be wrapped round the body, and all the flow between the shock wave and the body would be compressed into a layer of negligible thickness. (Note that here viscosity and allied effects are neglected; their importance can be gauged better when a second approximation has yielded an estimate of the thickness of this 'compressed-air cap'.)

Now, since by (34) for $K = \infty$ the pressure immediately behind a shock wave is $\rho_0 V^2 \sin^2\eta$, while, if the shock wave is wrapped closely round the body, $\eta = \chi$ at any point, it might be thought that the 'Newtonian' pressure distribution $\rho_0 V^2 \sin^2\chi$ would be recovered in the limit as $K \to \infty$. This neglects, however, the centrifugal pressure change across the layer, in which a large mass-flow moves with large velocity along streamlines with curvature equal to that of the body. The true surface pressure for $K = \infty$ is accordingly less than the Newtonian value. This calculation is briefly illustrated for a body of revolution in axisymmetric flow in § 3.6 (see Grimminger, Williams & Young (1950) for a more general discussion); some further details found by Freeman (1956) for this case are also described.

3.6. *Higher approximations: summary of Freeman's analysis for bodies of revolution*

If r signifies distance from the axis of symmetry, and (x, y) are the usual boundary-layer coordinates (x = distance along meridian section of surface, y = distance normal to surface), and the relationship between r and x on the surface is $r = R(x)$, and ψ is a Stokes stream function, whose value at each point is $(2\pi)^{-1}$ times the mass flow across a disc (coaxial with the body) with the point on its rim, then in the uniform flow upstream of the shock wave $\psi = \frac{1}{2}\rho_0 V r^2$, and so on the shock wave (which coincides with the body surface for $K = \infty$) $\psi = \frac{1}{2}\rho_0 V R^2(x)$. The angle $\chi(x)$ between the tangent plane and the axis is $\sin^{-1}R'(x)$. But the equation of momentum normal to the surface gives

$$\left(-\frac{d\chi}{dx}\right)\rho v^2 = \frac{\partial p}{\partial y} = \rho v r \frac{\partial p}{\partial \psi} = \rho v R(x) \frac{\partial p}{\partial \psi}, \tag{55}$$

since $-d\chi/dx$ is the curvature of the streamlines and since $\partial\psi/\partial y = \rho vr$. Here, inertia of flow normal to the surface is neglected, because the flow becomes purely tangential as $K \to \infty$. But the pressure at the shock wave was shown to be $\rho_0 V^2 \sin^2\chi(x)$; hence, the pressure at an arbitrary point behind it (that is, for any value of $\psi < \frac{1}{2}\rho_0 VR^2(x)$) is

$$p = \rho_0 V^2 \sin^2\chi + \frac{d\chi/dx}{R(x)} \int_{\psi}^{\frac{1}{2}\rho_0 V^2 R(x)} v \, d\psi. \tag{56}$$

The surface pressure is obtained from (56) by putting $\psi = 0$.

One still has the problem of selecting the value of v as a function of ψ for given x to be put in the integral. Here the properties of isentropic flow along streamlines are used. The streamline specified by ψ passed through the shock wave at the point $x = x_1$, say, where $\psi = \frac{1}{2}\rho_0 VR^2(x_1)$. At this point, by (34) with $K = \infty$, $i = \frac{1}{2}V^2 \sin^2\chi(x_1)$. Now, equation (44) shows that as $K \to \infty$ the change in i with changes in p becomes negligibly slow, so that in this limit we may take

$$v = \sqrt{(V^2 - 2i)} = V \cos\chi(x_1) \tag{57}$$

all along the streamline in question. Then (56), with its variable of integration changed from ψ to x_1, becomes

$$p = \rho_0 V^2 \left\{ \sin^2\chi(x) + \frac{\chi'(x)}{R(x)} \int_{x_1}^{x} R(x_1) R'(x_1) \cos\chi(x_1) \, dx_1 \right\}, \tag{58}$$

whence the surface pressure in the form given by Ivey, Klunker & Bowen (1948) is derived by putting $x_1 = 0$.

The approximations involved in this formula are as follows.

(i) The shock wave angle η has been taken equal to the body surface angle χ, although for convex bodies $\eta > \chi$.

(ii) The streamline curvature has been taken equal to that of the body, although it will be less for convex bodies.

(iii) The increase in velocity along a streamline as the pressure falls has been neglected.

(iv) The terms in $1/K$ and $1/K^2$ in the shock equations (34) have been neglected.

(v) The pressure gradient normal to the wall has been taken equal to the (centrifugal) pressure gradient normal to the streamlines, although since the streamlines are not exactly parallel to the wall it must contain a component of the streamwise pressure gradient as well.

Of these, approximations (i) and (ii) tend to underestimate the surface pressure, and (iii) and (iv) to overestimate it. Approximation (v) can work either way, but is probably the least important of the five. Since the experiments of Oliver (1956), although performed at Mach numbers at which the strong-shock approximation is in error by 15%, and under conditions in which air behaves like an ideal diatomic gas, with $K = 6$ (obviously too low a value for the approximations to be good), give surface pressures consistently greater than equation (58) predicts, and in fact

close to Lees's equation (54), we may infer that approximations (i) and (ii) are more seriously in error than (iii) and (iv). Probably the order of importance of the errors involved in the different approximations is that given in the list.

Attempts have sometimes been made (e.g. by Grimminger *et al.* 1950) to produce better agreement with experiment by choosing a different relation between v and ψ to insert in (56), but this clearly requires v to *decrease* along streamlines, although the pressure is falling. Viscous action could explain this, but hardly at the Reynolds numbers of the experiments. Probably approximations (i) and (ii) are a much more important source of error at fairly low values of K. All the sources of error will, however, decrease as K becomes greater.

In addition to the experimental disagreement, the theory contains within itself signs of its own limitations. For certain shapes, the surface pressure falls to zero for some x. Thus, for a sphere of radius a, $R(x) = a\sin(x/a)$ and $\chi(x) = \frac{1}{2}\pi - x/a$ and the surface pressure given by (58) is

$$p = \rho_0 V^2\{1 - \tfrac{4}{3}\sin^2(x/a)\}, \tag{59}$$

which vanishes at $x/a = \frac{1}{3}\pi$, that is, at 60° from the front stagnation point. Ivey, Klunker & Bowen (1948) suggest that the flow separates from the surface at this point, leaving a dead-air region near the surface in which the pressure coefficient is negligible. They calculate the drag of a sphere on this basis as two-thirds of the 'Newtonian' value.

The present author does not believe that the flow separates from the surface at this point, even for very large K, but rather that the *shock wave* separates from the surface there. The assumption of very small streamtube area then breaks down, because in hypersonic flow enormous increases in streamtube area are possible when the pressure has fallen by a large factor (and it must ultimately fall to at least its upstream value). The whole approximation thus becomes non-uniformly valid as the point of shock wave separation is approached.

This hypothesis is borne out by the behaviour of the second approximation (Freeman 1956) to the Ivey, Klunker & Bowen theory. Freeman first finds y as a function of x along each streamline $\psi =$ constant by integrating

$$y = \frac{\rho_0}{R(x)}\int_0^{\psi}\frac{d\psi}{\rho v}, \tag{60}$$

in which he takes v as given by (57), and, since γ is so near 1 for K large (§ 3.4),

$$\rho \doteqdot \rho_1\frac{p}{p_1} = \frac{K(x_1)p}{V^2\sin^2\chi(x_1)}, \tag{61}$$

with p given by (58). Here, $K(x_1)$ stands for the value of K at a shock whose angle of inclination to the oncoming flow is $\chi(x_1)$. Hence, the equation of the streamline is

$$y = \frac{1}{R(x)}\int_0^{x_1}\frac{R(x_1)\,R'(x_1)\sin^2\chi(x_1)\,dx_1}{K(x_1)\cos\chi(x_1)\left\{\sin^2\chi(x) + \dfrac{\chi'(x)}{R(x)}\displaystyle\int_{x_1}^{x} R(x_1)\,R'(x_1)\cos\chi(x_1)\,dx_1\right\}}, \tag{62}$$

where x_1 as before is the position where the streamline passes through the shock wave. Note that the distance of the streamline from the surface is of order K^{-1}; however, where the pressure p begins to be small, the coefficient of K^{-1} starts to increase rapidly.

The integral (62) converges at its lower limit because $R(x_1)$ tends to 0 as well as $\cos\chi(x_1)$ as $x_1 \to 0$. Otherwise (as happens in the corresponding theory (Chester 1956, Freeman 1956) for two-dimensional flow) one would have to use a better approximation to v than (57) for small x_1 (i.e. very near the body).

Freeman next obtains the equation $y = y_s(x)$ of the shock wave, by simply replacing the upper limit in (62) by x, so that it becomes the value of y for the streamline which passes through the shock wave at the point x itself. This expression again is of order K^{-1} but becomes large as the point of shock separation is approached. As $x \to 0$, on the other hand, it is easy to show that

$$y_s(x) \to a/K, \tag{63}$$

where $K = K(0)$ stands for its value at the normal part of the shock wave and a is the radius of curvature of the body at the nose. (It is interesting that this stand-off distance of the shock wave ahead of the body is exactly twice the value obtained by the very crude approximation of assuming irrotational flow behind the shock wave. Equation (63) is closer to the experimental results. A more accurate value than either will be found in § 3.9). Strictly, the assumptions of the theory break down near the stagnation point, since the flow velocities are not even approximately tangential there, but Freeman (1956) is able to take approximate account of the normal components of velocity in this region, and to show that they do not affect the equation $y = y_s(x)$ of the shock wave to the approximation used. This analysis shows also that in this region, for K large, the tangential velocity component v_x falls linearly with y from its value V_x/a on the shock wave to zero on the body, a striking result which would restrict greatly the importance of viscosity if it were true, and which also will be critically evaluated in § 3.9.

He then goes on to obtain the surface pressure distribution to a second approximation, in which all the effects numbered (i) to (v) above are taken into account, by use of the shock shape and streamline shapes which have just been obtained, and an increase of velocity along a streamline which corresponds to the pressure fall as calculated on the first approximation. To the second approximation thus obtained, the pressure starts at the correct stagnation-point value (53), which is below the first approximation, and for a sphere (for which numerical details are obtained) begins to rise above the first approximation for $\theta > 20°$, and has already diverged very greatly from its first approximation when $\theta = 45°$.

It is clear from this that the whole process diverges near the point of shock separation, largely because the assumption of small streamtube area behind the shock wave starts to break down when the pressure has fallen

by a factor at all comparable with the shock-density ratio K. (The breakdown occurs even sooner in two-dimensional flow.)

Chester (1956) gets similar results to Freeman in a method of successive approximation in which the shape of the shock wave is taken as given and the shape of the body progressively determined. He uses a perfect gas with constant specific heats but pushes the calculations to one degree of approximation higher than those of Freeman.

3.7. *Bodies of revolution with shock wave separation at the base*

It must now be noticed that many bodies of revolution terminate in a flat base in such a way that no shock wave separation occurs until the base is reached—either because the angle χ between the surface and the stream remains fairly large ahead of the base, or because as χ falls the curvature $(-d\chi/dx)$, and with it the centrifugal pressure drop, falls also.

For example, on a paraboloid of revolution whose equation in cylindrical polar coordinates (r, z) is $r^2 = 2az$ (here, as in § 3.6, a is the radius of curvature at the nose), the pressure given by the Ivey, Klunker & Bowen formula nowhere falls to zero. For, in cylindrical coordinates, that formula (§ 3.6) may be written

$$\frac{p}{\rho_0 V^2} = \frac{1}{1+(dz/dr)^2} - \frac{d^2z/dr^2}{r\{1+(dz/dr)^2\}^{3/2}} \int_0^r \frac{r(dz/dr)\,dr}{\{1+(dz/dr)^2\}^{1/2}}, \tag{64}$$

which for the paraboloid is easily evaluated as

$$\frac{p}{\rho_0 V^2} = \frac{1}{2}\left\{\frac{1}{1+(r/a)^2} + \frac{\sinh^{-1}(r/a)}{(r/a)\{1+(r/a)^2\}^{3/2}}\right\}. \tag{65}$$

Note that this is always more than half the simple 'Newtonian' value. At $r = a$, where $\chi = 45°$ (and the meridian radius of curvature has increased to $2{\cdot}83a$), $p/\rho_0 V^2$ has fallen to 0·406. The approximation is of doubtful value at pressures much below this, but there is not the same catastrophic failure of the theory as there was near the position on the sphere where the first approximation to p vanished.

Another example easily worked out by equation (64) is the body $r^3 = 3b^2z$, for which the radius curvature falls from *infinity* at the nose to a minimum of $1{\cdot}30b$ at $r = 0{\cdot}707b$ before rising again as r increases further (for example, it is $1{\cdot}41b$ when $r = b$ and $\chi = 45°$). The surface pressure distribution is

$$\frac{p}{\rho_0 V^2} = \frac{1}{\{1+(r/b)^4\}^{3/2}}, \tag{66}$$

giving $p/\rho_0 V^2 = 0{\cdot}354$ when $r = b$. Note that the pressure where $\chi = 45°$ is lower in this case than for the paraboloid, whose radius of curvature relative to the local value of r is twice as great at that point. The pressure at $\chi = 45°$ on a sphere is lower than either ($p/\rho_0 V^2 = 0{\cdot}333$), although the ratio of the local radius of curvature to r has the same value $\sqrt{2}$ as for the cubic shape. This is because the flow velocities at $\chi = 45°$ are smaller for the cubic shape, for which less of the fluid has passed through the more oblique parts of the shock.

For most other shapes, numerical integration is necessary in (64). One can get useful analytical expressions, however, for the purpose of seeing quickly how various kinds of variation of shape affect the pressure distribution, by studying bodies in which $\cos\chi$ is a simple function of r, using the form

$$\frac{p}{\rho_0 V^2} = 1 - \cos^2\chi - \frac{1}{r}\frac{d\cos\chi}{dr}\int_0^r (\cos\chi) r\, dr \tag{67}$$

of the Ivey, Klunker & Bowen formula. The general shape of the body is fairly obvious from the form of $\cos\chi$ as a function of r, and can be computed quickly from the formula $dz/dr = \cot\chi$.

One may use (67), for example, to discuss different ways of rounding the nose of a cone of given semi-angle χ_0. On the cone itself $p/\rho_0 V^2$ will be $\sin^2\chi_0$. If a spherical nose is used the pressure just before the conical part will be $1 - \frac{4}{3}\cos^2\chi_0$ to the first approximation. The sudden rise in pressure as the conical part is reached, although it will doubtless be smoothed out and reduced in magnitude a bit in the real flow (because the centrifugal effect does not cease instantly when the fluid reaches the conical part, and because the effect is overestimated in the Ivey, Klunker & Bowen formula), may cause undesirable boundary layer behaviour (instability, etc.). With a paraboloidal nose the pressure falls instead to

$$\tfrac{1}{2}(\sin^2\chi_0 + \sin^4\chi_0 \sec\chi_0 \sinh^{-1}\cot\chi_0),$$

for example (if $\chi_0 = 45°$) to 0·406 instead of 0·333, but the sudden rise to 0·5 may again be harmful. Instead, one can let the radius of curvature become infinite where the nose joins on the cone. Choosing

$$\cos\chi = \frac{r}{a} - \frac{r^2}{4a^2}\sec\chi_0, \tag{68}$$

which gives $\chi = \chi_0$ and $d\chi/dr = 0$ when $r = 2a\cos\chi_0$, we find from (67) that

$$\frac{p}{\rho_0 V^2} = 1 - \frac{4}{3}\left(\frac{r}{a}\right)^2 + \frac{35}{48}\left(\frac{r}{a}\right)^3 \sec\chi_0 - \frac{3}{32}\left(\frac{r}{a}\right)^4 \sec^2\chi_0. \tag{69}$$

This is continuous with $p/\rho_0 V^2 = \sin^2\chi_0$ at $r = 2a\cos\chi_0$, but falls to a minimum of $1 - 1{\cdot}055\cos^2\chi_0$ at $r = 1{\cdot}735a\cos\chi_0$, for example to a minimum of 0·473 if $\chi_0 = 45°$. Thus some slight pressure rise still occurs but it is much smaller and more gradual. The need for some pressure rise immediately before an accurately conical portion is easily seen by differentiating (67).

Conversely, equation (67) may be inverted, to give the shape of body with a given first approximation to the pressure distribution, as

$$\cos\chi = \frac{\displaystyle\int_0^r \left(1 - \frac{p_1}{\rho_0 V^2}\right) r_1\, dr_1}{\left\{\displaystyle\int_0^r \left(1 - \frac{p_1}{\rho_0 V^2}\right)(r^2 - r_1^2) r_1\, dr_1\right\}^{1/2}} \tag{70}$$

(which must be used with $dz/dr = \cot\chi$ if the body shape is to be plotted). Here p_1 is the pressure (to the first approximation) at the point $r = r_1$ on the surface.

For example, if one takes the pressure to be its value on a sphere of radius a up to a certain value of r, and thereafter constant and equal to that on a cone of semi-angle χ_0, in other words if

$$\left.\begin{aligned} \frac{p_1}{\rho_0 V^2} &= 1 - \frac{4}{3}\left(\frac{r}{a}\right)^2 \qquad (r < a\tfrac{1}{2}\sqrt{3}\cos\chi_0), \\ &= \sin^2\chi_0 \qquad\qquad (r > a\tfrac{1}{2}\sqrt{3}\cos\chi_0), \end{aligned}\right\} \tag{71}$$

then (70) gives

$$\left.\begin{aligned} \cos\chi &= r/a \qquad\qquad\qquad\qquad\qquad\qquad (r < a\tfrac{1}{2}\sqrt{3}\cos\chi_0), \\ &= \cos\chi_0\left\{1 + \frac{\frac{3}{64}a^4\cos^4\chi_0}{(r^2 - \frac{3}{8}a^2\cos^2\chi_0)^2}\right\}^{-1/2} \qquad (r > a\tfrac{1}{2}\sqrt{3}\cos\chi_0). \end{aligned}\right\} \tag{72}$$

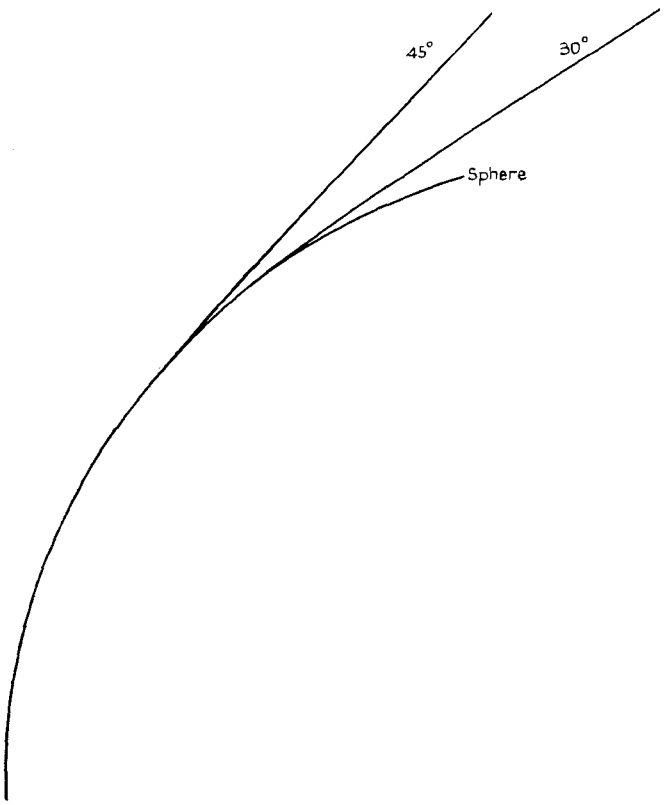

Figure 4. Transition curves from spherical nose to cones of semi-angles 45° and 30°. Bodies of revolution with these meridian sections would have constant surface pressure behind the spherical portion, according to the Ivey, Klunker & Bowen formula (67).

It is to be noted how rapidly $\chi \to \chi_0$ as r increases; the transition from sphere to cone is made fast, although without the pressure dropping below its final value. The shape is plotted for $\chi_0 = 45°$ and $\chi_0 = 30°$ in figure 4. These are probably rather suitable 'transition curves' from the spherical to the conical shape, since the fact that the pressure formula overestimates the centrifugal effect can only mean that the tendency to pressure rise, already eliminated by the shape chosen, is less marked even than was assumed in the calculation.

3.8. *Shape of shock wave beyond where it separates from the body*

Both for bodies from which the shock wave separates at the base, and for those from which it is thrown off (as it were) by centrifugal force at a point ahead of the base, it is of interest to investigate the shape of the shock wave beyond where it separates. The following rather crude approximate treatment of this problem is based, as in §§ 3.6 and 3.7, on assuming K large.

For $K = \infty$ the shock wave coincides with the body up to the position of shock separation, and all the streamlines coincide with both shock and body. After shock separation, however, it seems likely that most of the streamlines will remain close to the shock rather than to the body, for when the shock is oblique the streamtubes passing through it are greatly reduced in area and lie closely parallel to it, and, also, all those streamtubes on which the pressure has not fallen off greatly from its value at the shock will still have a small streamtube area. If the shock has not become too oblique to the flow, then most of the mass flow inside it must flow along these streamtubes. The streamtubes nearest the body or wake, however, must have a low pressure, either because the wake is at a low 'base' pressure or because a large streamtube expansion in this region is necessary to fill up the growing space between the shock wave and the body. This suggests that the shock wave has such a shape that the centrifugal pressure drop, across streamlines most of which nearly coincide with it, reduces the pressure from its value at the shock to practically zero on the other side of those streamlines. This gives

$$0 = \rho_0 V^2 \sin^2\eta + \frac{d\eta/dx}{r_s(x)} \int_0^x v \, d\psi$$

$$= \rho_0 V^2 \left(\sin^2\eta + \frac{d\eta/dx}{r_s(x)} \int_0^x r_s(x_1) r_s'(x_1) \cos\eta(x_1) \, dx_1 \right), \tag{73}$$

where x is now a coordinate measured along the shock instead of along the body surface, $r_s(x)$ is the value of r at the shock, and the streamline curvature has now been taken equal to the shock wave curvature $(-d\eta/dx)$. Because $r_s'(x) = \sin\eta$, this equation may be written

$$r_s \sin\eta \frac{dr_s}{d\eta} + \int_0^{r_s} r_s \cos\eta \, dr_s = 0, \tag{74}$$

an equation which is easily solved after differentiation with respect to η as

$$r_s \sin^2\eta \frac{dr_s}{d\eta} = \text{const.} = -\sin\eta_0 \int_0^{r_0} r_s \cos\eta \, dr_s, \tag{75}$$

where suffix zero signifies the position of shock wave separation. (To a first approximation, one may take $\eta = \chi$ and $r_s = R(x)$ on the right-hand side of (75), since the shock coincides with the body up to separation.) Next, integrating (75) again, we obtain

$$\tfrac{1}{2}(r_s^2 - r_0^2) = (\cot\eta - \cot\eta_0)\sin\eta_0 \int_0^{r_0} r_s \cos\eta \; dr_s \tag{76}$$

as the relation between η and r_s along the shock. (One may note that this is also derivable, less simply, from (70) by putting $p_1 = 0$ for $r_1 > r_0$ and interpreting χ as η.)

The shock shape in cylindrical polar coordinates (r, z) is easily deduced from (76), because $dz_s/dr_s = \cot\eta$. Hence

$$z_s = z_0 + (r_s - r_0)\cot\eta_0 + \frac{\frac{1}{6}r_s^3 - \frac{1}{2}r_s r_0 + \frac{1}{3}r_0^3}{\sin\eta_0 \int_0^{r_0} r_s \cos\eta \; dr_s}, \tag{77}$$

showing that the approximate shock shape calculated in this way is a cubic.

The errors in this formula are similar to those enumerated after equation (58), except that (i) is absent; no error has been made in the shock wave angle in equation (73). However, the error in the streamline curvature may be more severe in this case. The streamlines near the body or wake are probably considerably more curved than the shock wave, indicating that (77) probably overestimates the curvature needed in the shock wave. One may hope, however, that their contribution to $\int v \, d\psi$ is only moderate because neither v nor the change in ψ across those streamlines can be very large. At present it does not seem clear how the theory beyond shock separation can be extended to a second approximation. However, in cases where separation occurs at the base, one may use Freeman's calculation of the second approximation to the shock shape up to separation, and take z_0, r_0, η_0 in (77) as the coordinates and angle of the shock wave at separation, and thus considerably improve the accuracy of (77) beyond separation.

When separation occurs before the base, the theory is less satisfactory because for any finite K a substantial departure of the shock wave from the body surface occurs before the theoretical position of separation, and Freeman's second approximation is of no value for calculating the later stages of this process. In these cases, the first approximation to the shock shape is put forward here principally because it might serve as the foundation of a future method of successive approximation, based (as is necessary for success) on a uniformly valid first approximation.

Figure 5 shows the shock wave shapes for separation from a spherical cap subtending a half-angle at the centre of 10°, 20°, 30°, 40°, 50° and 60°; for convenience of comparison they are all superimposed on a single figure, and the values for $K = \infty$ only have been plotted. The first three are likely to have more value than the others; for finite K these may well be close to the true shock shape if the body is taken to be a portion of a sphere concentric with the spherical part of the shock but of a smaller radius (to

be determined in § 3.9; the position of such an inner sphere for $K = 15$, 12, 9, 6 is noted on the figure). The last of the shock shapes shown is a very crude first approximation, for large K, to the shape of the shock wave on a complete sphere (which separates from the surface at $\chi = 30°$).

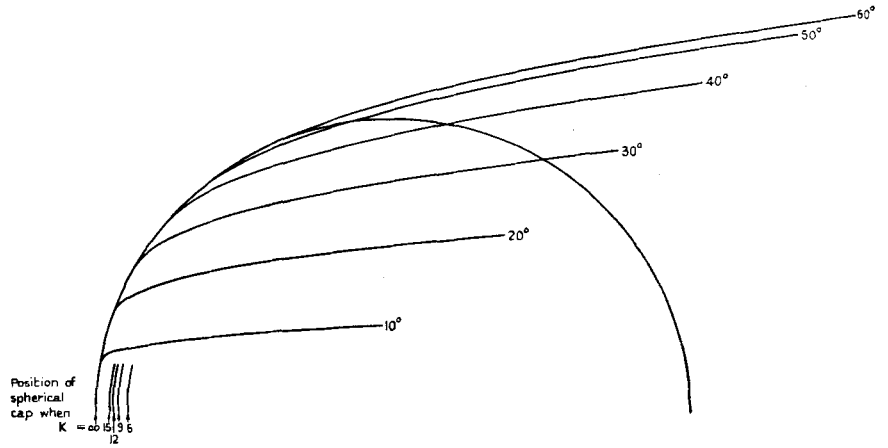

Figure 5. Shapes of shock waves trailing behind spherical caps subtending semi-angles 10°, 20°, 30°, 40°, 50°, 60° at their (common) centre.

3.9. *Constant-density approximation to flow near front stagnation point*

An approximation for use in the neighbourhood of the front stagnation point (a region important for heat transfer since the fluid temperature is greatest there and the boundary layer thinnest) is now obtained without any procedure of successively discarding inverse powers of K. It can be used to check some aspects of theories based on those procedures.

The present approximation is based instead on the theory of incompressible flow; thus it neglects variations of density, both (i) along the back of the shock wave—this is permissible wherever η does not vary much from $\frac{1}{2}\pi$, in which case $v_{n0} = V \sin\eta$ cannot vary enough to produce any significant variation of $K = \rho_1/\rho_0$—and (ii) along streamlines behind the shock wave—this confines us to regions in which the velocity does not approach close to the local speed of sound. Both assumptions should be adequate in the region behind that part of the shock wave in which η varies between 80° and 90°.

The body shape in the region of interest is taken to be part of a sphere of radius a, since bodies with at least a spherical portion of surface near the nose are of great interest. For other bodies of revolution, however, the theory could reasonably be applied with a as a mean radius of curvature of the surface in the region just described.

Taking incompressible flow behind the shock wave, and K constant in the boundary conditions at the shock wave, we shall show that all the equations of motion and boundary conditions can be satisfied by assuming

a spherical shock of radius $c > a$. We use spherical polar coordinates (r, θ, λ) with the line $\theta = 0$ pointing upstream, and a Stokes stream function ψ such that

$$\frac{\partial \psi}{\partial r} = (r \sin\theta) v_\theta, \qquad \frac{\partial \psi}{\partial \theta} = -(r^2 \sin\theta) v_r, \tag{78}$$

where the suffixes on the v's signify components.

On the spherical shock wave, by (27) and (28),

$$v_r = -\frac{V \cos\theta}{K}, \qquad v_\theta = V \sin\theta, \tag{79}$$

and these conditions are satisfied if

$$\psi = \frac{Vc^2 \sin^2\theta}{2K}, \qquad \frac{\partial \psi}{\partial r} = Vc \sin^2\theta \quad \text{on } r = c. \tag{80}$$

In axisymmetrical flow the only component of vorticity is

$$\omega_\lambda = \frac{1}{r}\frac{\partial (r v_\theta)}{\partial r} - \frac{1}{r}\frac{\partial v_r}{\partial \theta} = \frac{1}{r \sin\theta}\frac{\partial^2 \psi}{\partial r^2} + \frac{1}{r^3}\frac{\partial}{\partial \theta}\left(\operatorname{cosec}\theta \frac{\partial \psi}{\partial \theta}\right). \tag{81}$$

But on the shock wave, by (43),

$$\omega_\lambda = \frac{(K-1)^2}{K}\frac{V \sin\theta}{c}. \tag{82}$$

Further, in axisymmetrical flow, the ratio $\omega_\lambda/(r \sin\theta)$ remains constant along each streamline, since the intensity of each vortex ring changes during convection in proportion to its radius. But since

$$\frac{\omega_\lambda}{r \sin\theta} = \frac{(K-1)^2 V}{Kc^2} \tag{83}$$

on the shock wave, and all the streamlines pass through the shock wave, the ratio must have this constant value everywhere.

Hence, by (81),

$$\frac{\partial^2 \psi}{\partial r^2} + \frac{\sin\theta}{r^2}\frac{\partial}{\partial \theta}\left(\operatorname{cosec}\theta \frac{\partial \psi}{\partial \theta}\right) = \frac{(K-1)^2}{K}\frac{Vr^2 \sin^2\theta}{c^2} \tag{84}$$

everywhere. This equation will now be solved subject to the boundary conditions (80), and it will be shown that the dividing streamline is a sphere of radius $r = a < c$. (Note that no boundary condition on the pressure need be applied at the shock wave; the equation of motion determines the pressure once the velocity field is known, and the condition (43) on the vorticity was obtained as the condition that the boundary condition on the pressure is compatible with the equation of motion.)

The solution of (84) under the boundary conditions (80) takes the form

$$\psi = \Psi(r) \sin^2\theta, \tag{85}$$

where

$$\Psi''(r) - \frac{2}{r^2}\Psi(r) = \frac{(K-1)^2}{K}\frac{Vr^2}{c^2}, \tag{86}$$

and

$$\Psi(c) = \frac{Vc^2}{2K}, \qquad \Psi'(c) = Vc. \tag{87}$$

The function $\Psi(r)$ satisfying these conditions is easily found to be

$$\Psi(r) = \frac{Vc^2}{30K}\left\{3(K-1)^2\left(\frac{r}{c}\right)^4 - 5K(K-4)\left(\frac{r}{c}\right)^2 + 2(K-1)(K-6)\left(\frac{r}{c}\right)^{-1}\right\}. \tag{88}$$

The solution given by (85) and (88) shows that the streamline $\psi = 0$ divides at $r = a$, the greatest root of $\Psi(r) = 0$ which is less than c. (It can be shown that roots of $\Psi(r) = 0$ with $0 < r < c$ exist for all $K > 1$.) The streamline then continues along the sphere $r = a$, and hence the flow may be regarded as the flow about a solid sphere of radius a.

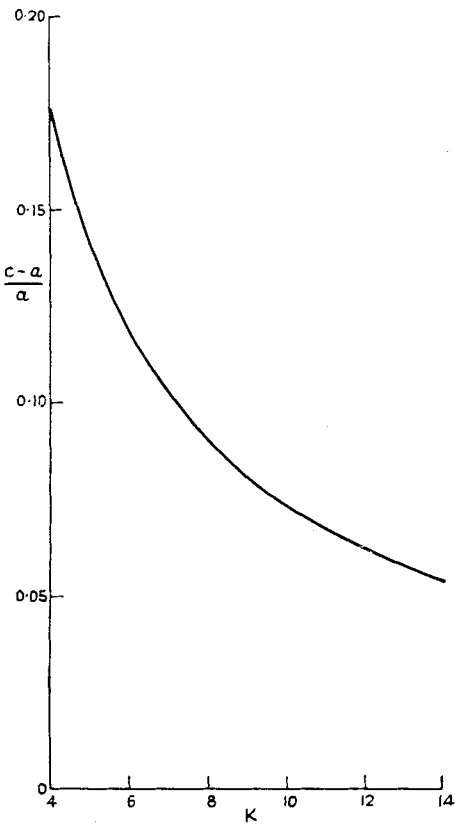

Figure 6. Ratio of stand-off distance of shock wave ahead of sphere at radius of sphere, as a function of K.

Particular interest attaches to $(c-a)/a$, the 'stand-off distance' of the shock wave as a fraction of the radius of the sphere. This is a function of K alone, a graph of which for $K \geqslant 4$ (an inequality which by the physical significance of K must be satisfied for all gases) is given in figure 6.

One is interested also in the distribution of v_θ between the shock wave and the sphere. By (78),

$$\frac{v_\theta}{V\sin\theta} = \frac{\Psi'(r)}{Vr}. \tag{89}$$

This is plotted against r/c for a number of values of K in figure 7. The flow is seen to be in nearly (though not exactly) uniform shear, as predicted by Freeman's first approximation (§ 3.6), but the velocity at the wall is not zero as that approximation would give. Freeman's second approximation to the velocity at the wall (derived from Bernoulli's equation and the Ivey, Klunker & Bowen value of the pressure) is, however, accurate to within 1% for all the K's shown. Putting this a different way, the pressure on the surface derived from (89) is

$$p = \rho_0 V^2 \left\{1 - \frac{1}{2K} - (\tfrac{4}{3} \pm 0{\cdot}01)\sin^2\theta\right\}; \tag{90}$$

that is, the maximum departure of the coefficient of $\sin^2\theta$ from the Ivey, Klunker & Bowen value $\frac{4}{3}$ for $K \geqslant 4$ is 0·01.

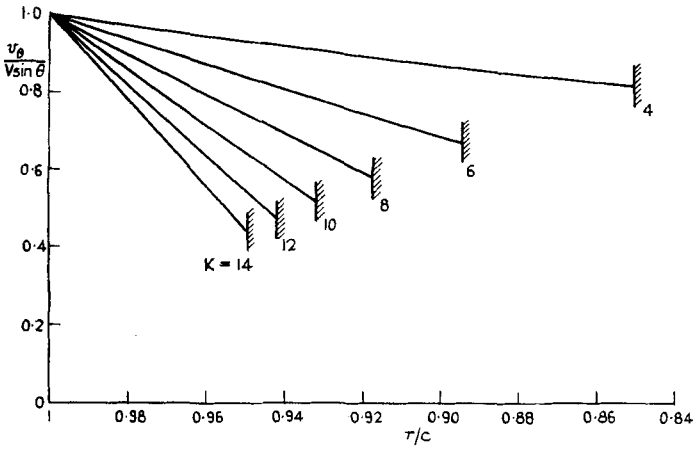

Figure 7. Distribution of transverse velocity v_θ in the nose region of the flow around a sphere, plotted for different values of K (the density-ratio across the normal part of the shock wave). The coordinate r (the distance from the centre of the sphere) takes the value c at the shock wave; the position of the body surface ($r = a$) in each case is shown by hatching.

This agreement in the rate of pressure drop along the surface, near the nose, between two very dissimilar theories (the present one, which only approximates by taking the density constant, and the Ivey, Klunker & Bowen theory, which allows density variation but assumes large K, and hence a large reduction in streamtube area behind the shock wave) gives some added support to both, and makes one reasonably confident about the general view of equilibrium flow around bluff bodies, in the region where pressure is not a small fraction of $\rho_0 V^2$, presented in this § 3. What should be done to treat the flow where, as a result of the pressure falling by a large factor, the streamtube area becomes large again, remains at present a mystery.

References

BRITTON, D., DAVIDSON, N. & SCHOTT, G. 1954 *Disc. Faraday Soc.* **17**, 58.

BUSEMANN, A. 1933 *Handwörterbuch der Naturwissenschaften*, 2^{e} Auflage, p. 276. Jena : Gustav Fischer.

CHESTER, W. 1956 *J. Fluid Mech.* **1**, 353 and 490.

FOWLER, R. H. & GUGGENHEIM, E. A. 1939 *Statistical Thermodynamics*. Cambridge University Press.

FREEMAN, N. C. 1956 *J. Fluid Mech.* **1**, 366.

GAYDON, A. G. 1953 *Dissociation Energies and Spectra of Diatomic Molecules*, 2nd Ed. London : Chapman and Hall.

GRIMMINGER, G., WILLIAMS, E. P. & YOUNG, G. B. W. 1950 *J. Aero. Sci.* **17**, 675.

HIRSCHFELDER, J. O., CURTISS, C. F. & BIRD, R. B. 1954 *Molecular Theory of Gases and Liquids*. New York : Wiley.

IVEY, H. R., KLUNKER, E. B. & BOWEN, E. N. 1948 *Nat. Adv. Comm. Aero., Wash., Tech Note* no. 1613.

LEES, L. 1955 *Hypersonic Flow*, Institute of Aeronautical Sciences, Washington, Preprint no. 554.

LIGHTHILL, M. J. 1956 *Surveys in Mechanics* (Ed. G. K. Batchelor & R. M. Davies), pp. 250–351. Cambridge University Press.

MORSE, P. M. 1929 *Phys. Rev.* **34**, 57.

NEWTON, I. 1687 *Principia Mathematica*, Book 2, Section 7.

OLIVER, R. E. 1956 *J. Aero. Sci.* **23**, 177.

PALMER, H. B. 1955 *J. Chem. Phys.* **23**, 2449.

VAN DYKE, M. D. 1954 *Nat. Adv. Comm. Aero., Wash., Tech. Note* no. 3173.